Comparison of the Addition of $CH_3^•$, $CH_2OH^•$, and $CH_2CN^•$ Radicals to Substituted Alkenes: A Theoretical Study of the Reaction Mechanism

Ming Wah Wong,*[1a,b] Addy Pross,*[1c,d] and Leo Radom*[1a]

Contribution from the Research School of Chemistry, Australian National University, Canberra, ACT 0200, Australia, Department of Chemistry, University of Queensland, Brisbane, QLD 4072, Australia, and School of Chemistry, University of Sydney, Sydney, NSW 2006, Australia

*Received November 18, 1993. Revised Manuscript Received February 9, 1994**

Abstract: High-level ab initio calculations at the QCISD/6-311G** + ZPVE level have been carried out to study the addition reactions of $CH_3^•$, $CH_2OH^•$, and $CH_2CN^•$ radicals to the substituted alkenes CH_2=CHX (X = H, NH_2, F, Cl, CHO, and CN) and the results analyzed with the aid of the curve-crossing model. We find that the reactivity of $CH_3^•$ is primarily governed by enthalpy effects, whereas both enthalpy and polar effects are important for the reactions of $CH_2OH^•$ and $CH_2CN^•$. There is no general barrier height–enthalpy correlation for the latter two radicals because of the presence in some cases of polar effects that stabilize the transition states without a corresponding stabilization of the products. The polar effects are not sufficient, however, to significantly shift the *location* of the transition states, so a general *structure*–enthalpy correlation is observed.

Introduction

The mechanism of radical addition to alkenes is a subject of great interest. In basic chemistry it represents a fundamental bond-forming process, while in applied chemistry it is of interest due to the fact that radical addition to alkenes is the central reaction in many polymer processes. Extensive mechanistic studies over many years have led to the conclusion that polar, steric, and enthalpy effects all play a key role in governing reactivity in these systems. However, it seems that for any given system, there remains considerable uncertainty regarding the relative importance of these individual factors.[2-4]

In a recent theoretical study[5] of the addition of methyl radical to monosubstituted alkenes (eq 1),

$$CH_3^• + CH_2{=}CHX \rightarrow CH_3CH_2CHX^• \quad (1)$$

we came to the surprising conclusion that the barrier to this process was primarily governed by enthalpy effects. Polar effects, long assumed to play a dominant role in methyl addition reactions, were found to be unexpectedly small; we found no evidence for the widely accepted view that methyl radical is generally nucleophilic in character.

Following the unexpected nature of the conclusions reached in our study of methyl radical addition to alkenes, we decided that it would be desirable to extend our work to examine the mechanism of addition reactions of representative *substituted* methyl radicals: in the first instance, $CH_2OH^•$, which would be expected to be nucleophilic in character compared with methyl, and $CH_2CN^•$, which would be expected to be electrophilic compared with methyl. Accordingly, we have studied the reactions

$$CH_2OH^• + CH_2{=}CHX \rightarrow HOCH_2CH_2CHX^• \quad (2)$$

and

$$CH_2CN^• + CH_2{=}CHX \rightarrow NCCH_2CH_2CHX^• \quad (3)$$

for a family of alkenes CH_2=CHX (X = H, NH_2, F, Cl, CHO, and CN). Through a combination of ab initio calculations[6] and an analysis of the reactions using the curve-crossing model,[7] we have sought (a) to compare the reactivity of $CH_2OH^•$ and $CH_2CN^•$ with that of $CH_3^•$, (b) to determine the importance of polar and enthalpic effects in the radical addition reactions of $CH_2OH^•$ and $CH_2CN^•$ and, together with the data for the reactions of $CH_3^•$, to build up a general picture of the relative importance of polar and enthalpy effects in radical addition reactions, and (c) to obtain general insights into the nature of the transition state in this fundamental organic reaction. We note that our calculations refer to reactivity in the gas phase.

Computational Procedures and Results

High-level ab initio calculations[6] were carried out using the GAUSSIAN 92 series of programs[8] for the reactants, products, and transition structures of reactions 1–3 with X = H, NH_2, F, Cl, CHO, and CN. Geometries were optimized and vibrational

* Abstract published in *Advance ACS Abstracts*, June 1, 1994.

(1) (a) Australian National University. (b) University of Queensland. (c) University of Sydney. (d) Permanent address: Ben-Gurion University of the Negev, Beer Sheva, Israel.

(2) For reviews, see: (a) Giese, B. *Angew. Chem., Int. Ed. Engl.* **1983**, *22*, 753. (b) Tedder, J. M. *Angew. Chem., Int. Ed. Engl.* **1982**, *21*, 401. (c) Tedder, J. M.; Walton, J. C. *Adv. Free Radical Chem.* **1980**, *6*, 155. For a recent thorough analysis of the mechanistic aspects of radical addition reactions, see: (d) Heberger, K.; Fischer, H. *Int. J. Chem. Kinet.* **1993**, *25*, 249.

(3) For recent experimental studies on the importance of polar effects in the addition reactions of substituted methyl radicals, see: (a) Munger, K.; Fischer, H. *Int. J. Chem. Kinet.* **1985**, *17*, 809. (b) Beranek, I.; Fischer, H. In *Free Radicals in Synthesis and Biology*; Minisci, F.; Ed.; Kluwer: Dordrecht, 1989. (c) Fischer, H. In *Free Radicals in Synthesis and Biology*; Viehe, H. G., Janousek, Z., Merenyi, R., Eds.; Reidel: Dordrecht, 1986. (d) Heberger, K.; Walbiner, M.; Fischer, H. *Angew. Chem., Int. Ed. Engl.* **1992**, *31*, 635. (e) Fischer, H.; Paul, H. *Acc. Chem. Res.* **1987**, *20*, 200. (f) Avila, D. V.; Ingold, K. U.; Lusztyk, J.; Dolbier, W. R.; Pan, H.-Q. *J. Am. Chem. Soc.* **1993**, *115*, 1577. (g) Citterio, A.; Sebastiano, R.; Marion, A.; Santi, R. *J. Org. Chem.* **1991**, *56*, 5328. (h) Riemenschneider, K.; Bartels, H. M.; Dornow, R.; Drechsel-Grau, E.; Eichel, W.; Luthe, H.; Matter, Y. M.; Michaelis, W.; Boldt, P. *J. Org. Chem.* **1987**, *52*, 205. (i) Reference 2d.

(4) For recent theoretical studies on the addition of methyl and substituted methyl radicals to alkenes, see: (a) Zipse, H.; He, J.; Houk, K. N.; Giese, B. *J. Am. Chem. Soc.* **1991**, *113*, 4324. (b) Houk, K. N.; Paddon-Row, M. N.; Spellmeyer, D. C.; Rondan, N. G.; Nagase, S. *J. Org. Chem.* **1986**, *51*, 2874. (c) Fueno, T.; Kamachi, M. *Macromolecules* **1988**, *21*, 908. (d) Gonzales, C.; Sosa, C.; Schlegel, H. B. *J. Phys. Chem.* **1989**, *93*, 2435; **1989**, *93*, 8388. (e) Arnaud, R.; Vidal, S. *New J. Chem.* **1992**, *16*, 471. (f) Arnaud, R.; Subra, R.; Barone, V.; Lelj, F.; Olivella, S.; Sole, A.; Russo, N. *J. Chem. Soc., Perkin Trans. 2* **1986**, 1517. (g) Arnaud, R. *New J. Chem.* **1989**, *13*, 543. (h) Clark, T. *J. Chem. Soc., Chem. Commun.* **1986**, 1774. (i) Tozer, D. J.; Andrews, J. S.; Amos, R. D.; Handy, N. C. *Chem. Phys. Lett.* **1992**, *199*, 229. (j) Schmidt, C.; Warken, M.; Handy, N. C. *Chem. Phys. Lett.* **1993**, *211*, 272.

(5) (a) Wong, M. W.; Pross, A.; Radom, L. *J. Am. Chem. Soc.* **1993**, *115*, 11050. (b) Wong, M. W.; Pross, A.; Radom, L. *Isr. J. Chem.* **1993**, *33*, 415.

(6) Hehre, W. J.; Radom, L.; Schleyer, P. v. R.; Pople, J. A. *Ab Initio Molecular Orbital Theory*; Wiley: New York, 1986.

(7) For reviews of the curve-crossing model, see: (a) Pross, A.; Shaik, S. S. *Acc. Chem. Res.* **1983**, *16*, 363. (b) Pross, A. *Adv. Phys. Org. Chem.* **1985**, *21*, 99. (c) Shaik, S. S. *Prog. Phys. Org. Chem.* **1985**, *15*, 197. (d) Shaik, S. S. *Acta Chem. Scand.* **1990**, *44*, 205. (e) Shaik, S. S.; Schlegel, H. B.; Wolfe, S. *Theoretical Aspects of Physical Organic Chemistry, The S_N2 Transition State*; Wiley: New York, 1992.

0002-7863/94/1516-6284$04.50/0

frequencies determined at the UHF/6-31G* level. A variety of conformations, generated by internal rotation about single bonds in the transition structures and product radicals, were considered, and subsequent calculations were performed on the lowest energy forms. Reactions barriers and enthalpies were obtained through calculations using the quadratic configuration interaction procedure, QCISD,[9] and the additivity approximation:

$$\Delta E(\text{QCISD/6-311G**}) \approx \Delta E(\text{QCISD/6-31G*}) + \Delta E(\text{RMP2/6-311G**}) - \Delta E(\text{RMP2/6-31G*}) \quad (4)$$

Restricted open-shell second-order Møller–Plesset (RMP2) calculations[10] were employed within the additivity scheme. Zero-point vibrational energies (ZPEs) were obtained from the HF/6-31G* vibrational frequencies, scaled by a factor of 0.8929.[11] Unless otherwise noted, the barriers and enthalpies referred to in the text correspond to such QCISD/6-311G**//UHF/6-31G* + ZPE values. This represents the highest level of theory applied to date to study reactions 2 and 3. We have previously examined[5] reaction 1 at the QCISD(T)/6-311G**//UHF/6-31G* + ZPE level, but this was not feasible for the larger systems involved in reactions 2 and 3. However, we have found[12] that QCISD, in contrast to several other commonly used methods, smoothly mirrors the trends obtained with the more reliable QCISD(T) method. We have also found[12] that barriers obtained using UHF/6-31G* geometries are satisfactorily close to those obtained using QCISD/6-31G* geometries, even for strongly spin-contaminated cases. The extent of charge transfer between the radical and the alkene in the transition state was calculated at the UHF/6-31G* level using both the Mulliken and the Bader[13] methods, with the latter employing the PROAIM program.[14] Adiabatic ionization energies (I) and electron affinities (A) for the $CH_2OH^\bullet$ and $CH_2CN^\bullet$ radicals and for the set of alkenes (CH_2=CHX) were obtained at the G2(MP2) level of theory.[15] This corresponds effectively to calculations at the QCISD(T)/6-311+G(3df,2p) level, together with zero-point vibrational and isogyric corrections.

Calculated total energies and zero-point vibrational energies are presented in Table 1, while corresponding optimized geometries are available in the form of printed Gaussian archive files as supplementary material. Some of the more important structural features for the transition states for the radical addition reactions, shown schematically in Figure 1, are listed in Table 2. Barrier heights and reaction enthalpies for the three sets of reactions are listed in Table 3. Ionization energies, electron affinities and related data are presented in Table 4, while calculated charges are given in Table 5.

Discussion

Comparison of Theoretical and Experimental Data. It is important to assess the likely reliability of the various quantities calculated in the present study. Previous work[4,5,12] has shown that computed barriers for radical additions to alkenes are very sensitive to the level of theory employed. This need not necessarily be a problem in the present study since we are mainly concerned with *trends* in barrier values for different substituents. However, in a recent detailed study,[12] we found that even the trends in the barriers for the addition of methyl radical to a range of substituted ethylenes varied dramatically among many of the commonly used procedures. We concluded that great care must be taken in the selection of method in order to obtain meaningful results, *even* if only the trends in the barrier values are required. Among the theoretical procedures that we examined (UHF, ROHF, UMPn, RMPn, PMPn, QCISD, QCISD(T)) in our recent study,[12] we considered the QCISD(T) procedure to be the most reliable. We found that the trends in barriers obtained with QCISD(T) were reliably reproduced at the QCISD level and hence have employed that level of theory here. In support of this approach, we note that a comparison of results for the barrier to methyl radical addition obtained in the present study at the QCISD/6-311G** + ZPVE level with our previous results[5] obtained at the QCISD-(T)/6-311G** + ZPVE level shows differences between the two levels in the narrow range 3.7–4.6 kJ mol^{-1} for the set of substituents examined. For the reaction enthalpies, the differences between the two levels lie in the range 0.7–1.6 kJ mol^{-1}. Thus, the changes with substituent in barrier height and reaction enthalpy are indeed very similar at the QCISD and QCISD(T) levels. For the parent reaction of methyl radical plus ethylene, the QCISD/6-311G** + ZPVE barrier of 38.9 kJ mol^{-1} at 0 K (Table 3) may be compared with the experimental barrier (corrected to 0 K)[5b,16] of 38.2 kJ mol^{-1}. The QCISD/6-311G** + ZPVE exothermicity of 93.5 kJ mol^{-1} at 0 K is close to the experimental exothermicity[17] of 94.7 kJ mol^{-1}.

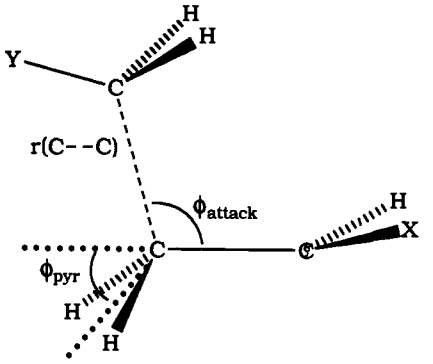

Figure 1. Schematic diagram showing key geometrical parameters in the transition state for the addition reaction of substituted methyl radicals ($CH_2Y^\bullet$) to substituted ethylenes (CH_2=CHX).

We have previously compared[5] the G2(MP2) ionization energies (I) for the alkenes CH_2=CHX with experimental values[17] and noted the good agreement between them. The mean absolute difference between theory and experiment was found to be 0.06 eV, with a maximum deviation of 0.12 eV. In the present study, we have calculated, in addition, G2(MP2) ionization energies for $CH_2OH^\bullet$ and $CH_2CN^\bullet$ of 7.43 and 10.16 eV (Table 4) that may be compared with experimental values[17] of 7.56 and 10.0 eV, respectively.

We have also previously noted[5] "reasonably satisfactory" agreement between the G2(MP2) and experimental[17,18] electron affinities (A) but expressed caution in the case of systems with negative A values. In the present work, we have calculated, in addition, the electron affinity for the $CH_2CN^\bullet$ radical, for which the G2(MP2) value of 1.59 eV is very close to recent experimental estimates[17] of 1.543–1.560 eV.

Description of the Curve-Crossing Model. The curve-crossing model may be used to build up the reaction profile for a radical

(8) Frisch, M. J.; Trucks, G. W.; Head-Gordon, M.; Gill, P. M. W.; Wong, M. W.; Foresman, J. B.; Johnson, B. G.; Schlegel, H. B.; Robb, M. A.; Replogle, E. S.; Gomperts, R.; Andres, J. L.; Raghavachari, K.; Binkley, J. S.; Gonzalez, C.; Martin, R. L.; Fox, D. J.; DeFrees, D. J.; Baker, J.; Stewart, J. J. P.; Pople, J. A. *GAUSSIAN 92*; Gaussian Inc.: Pittsburgh, PA, 1992.

(9) Pople, J. A.; Head-Gordon, M.; Raghavachari, K. *J. Chem. Phys.* **1987**, *87*, 5968.

(10) Knowles, P. J.; Andrews, J. S.; Amos, R. D.; Handy, N. C.; Pople, J. A. *Chem. Phys. Lett.* **1991**, *186*, 130.

(11) Curtiss, L. A.; Raghavachari, K.; Trucks, G. W.; Pople, J. A. *J. Chem. Phys.* **1991**, *94*, 7221.

(12) Wong, M. W.; Radom, L. To be published.

(13) Bader, R. F. W. *Atoms in Molecules. A Quantum Theory*; Oxford Press: New York, 1990.

(14) Biegler-Konig, F. W.; Bader, R. F. W.; Tang, T.-H. *J. Comput. Chem.* **1982**, *3*, 317.

(15) Curtiss, L. A.; Raghavachari, K.; Pople, J. A. *J. Chem. Phys.* **1993**, *98*, 1293.

(16) Kerr, J. A. In *Free Radicals*; Kochi, J., Ed.; Wiley: New York, 1972; Vol. 1.

(17) Lias, S. G.; Bartmess, J. E.; Liebman, J. F.; Holmes, J. L.; Levin, R. D.; Mallard, W. G. *J. Phys. Chem. Ref. Data* **1988**, *17*, Suppl. 1.

(18) Jordan, K. D.; Burrow, P. D. *Chem. Rev.* **1987**, *87*, 557, and references therein.

Table 1. Calculated Total Energies[a] (hartrees), Zero-Point Vibrational Energies[b] (ZPE, kJ mol^{-1}), and Spin-Squared Expectation Values (S^2)[b] Related to $CH_3^\bullet$, $CH_2OH^\bullet$, and $CH_2CN^\bullet$ Addition Reactions to CH_2=CHX

	X	total energy HF/6-31G*	RMP2/6-31G*	RMP2/6-311G**	QCISD/6-31G*	ZPE	S^2
				Radical			
$CH_3^\bullet$		−39.558 99	−39.668 46	−39.707 25	−39.688 87	81.3	0.76
$CH_2OH^\bullet$		−114.408 76	−114.695 55	−114.778 68	−114.717 56	105.6	0.76
$CH_2CN^\bullet$		−131.306 89	−131.685 52	−131.746 59	−131.706 98	84.8	0.92
				Alkenes (CH_2=CHX)			
	F	−176.881 95	−177.302 12	−177.415 65	−177.327 37	125.1	0.00
	H	−78.031 72	−78.284 34	−78.343 58	−78.312 38	143.8	0.00
	NH_2	−133.061 96	−133.477 24	−133.570 88	−133.510 08	194.9	0.00
	Cl	−536.933 69	−537.315 73	−537.399 38	−537.350 03	121.2	0.00
	CHO	−190.762 42	−191.308 49	−191.416 65	−191.340 36	174.5	0.00
	CN	−169.768 02	−170.292 72	−170.374 47	−170.319 66	144.3	0.00
				$CH_3^\bullet$ + CH_2=CHX TS			
	F	−216.424 34	−216.955 06	−217.108 67	−217.002 60	214.7	1.02
	H	−117.575 69	−117.937 45	−118.037 23	−117.987 74	234.1	1.03
	NH_2	−172.602 61	−173.131 57	−173.265 98	−173.186 10	284.9	1.00
	Cl	−576.479 54	−576.971 50	−577.095 64	−577.027 69	210.9	1.04
	CHO	−230.313 19	−230.967 94	−231.115 13	−231.020 35	262.5	1.19
	CN	−209.319 45	−209.953 08	−210.074 28	−210.000 70	231.7	1.17
				Product ($CH_3CH_2CHX^\bullet$)			
	F	−216.482 79	−217.019 53	−217.170 57	−217.062 60	233.4	0.76
	H	−117.631 72	−118.000 11	−118.097 42	−118.045 27	247.8	0.76
	NH_2	−172.661 71	−173.195 74	−173.327 33	−173.247 04	302.9	0.76
	Cl	−576.537 97	−577.036 25	−577.158 18	−577.088 56	228.4	0.76
	CHO	−230.375 70	−231.035 58	−231.179 96	−231.085 96	279.9	0.92
	CN	−209.381 75	−210.022 11	−210.141 20	−210.066 79	247.8	0.92
				$CH_2OH^\bullet$ + CH_2=CHX TS			
	F	−291.274 60	−291.984 09	−292.181 37	−292.032 09	234.0	1.03
	H	−192.425 87	−192.967 13	−193.110 87	−193.017 39	253.2	1.02
	NH_2	−247.452 33	−248.159 81	−248.338 01	−248.214 83	303.5	1.01
	Cl	−651.330 03	−652.001 48	−652.169 82	−652.057 74	229.9	1.03
	CHO	−305.163 71	−305.999 31	−306.190 65	−306.051 56	282.1	1.17
	CN	−284.170 54	−284.985 49	−285.150 74	−285.033 00	251.7	1.14
				Product ($HOCH_2CH_2CHX^\bullet$)			
	F	−291.330 30	−292.042 02	−292.236 75	−292.086 47	249.2	0.76
	H	−192.479 23	−193.022 75	−193.164 18	−193.069 20	264.6	0.76
	NH_2	−247.508 51	−248.217 03	−248.392 89	−248.269 69	319.2	0.76
	Cl	−651.385 51	−652.057 76	−652.223 84	−652.111 47	244.2	0.76
	CHO	−305.224 45	−306.059 59	−306.248 47	−306.111 18	296.8	0.91
	CN	−284.229 82	−285.044 74	−285.208 04	−285.090 70	263.9	0.92
				$CH_2CN^\bullet$ + CH_2=CHX TS			
	F	−308.167 38	−308.976 05	−309.152 21	−309.018 78	216.1	1.09
	H	−209.319 46	−209.958 10	−210.080 13	−210.003 78	235.5	1.10
	NH_2	−264.348 24	−265.158 14	−265.314 79	−265.205 79	286.7	1.06
	Cl	−668.221 84	−668.991 57	−669.138 50	−669.043 22	212.1	1.12
	CHO	−322.055 06	−322.984 64	−323.154 59	−323.035 15	263.6	1.30
	CN	−301.060 10	−301.969 36	−302.113 34	−302.014 21	232.4	1.27
				Product ($NCCH_2CH_2CHX^\bullet$)			
	F	−308.215 29	−309.023 23	−309.197 70	−309.066 40	233.0	0.76
	H	−209.365 59	−210.004 42	−210.124 94	−210.049 74	247.6	0.76
	NH_2	−264.395 79	−265.200 68	−265.355 58	−265.252 09	302.6	0.76
	Cl	−668.269 87	−669.039 77	−669.185 29	−669.092 08	228.0	0.76
	CHO	−322.109 01	−323.040 60	−323.208 79	−323.090 96	280.4	0.92
	CN	−301.112 29	−302.024 17	−302.166 75	−302.068 73	247.5	0.92

[a] Based on UHF/6-31G* geometry. [b] UHF/6-31G* values.

addition reaction.[19] The four principal valence-bond (VB) configurations that contribute to the ground-state wave function, DA, D^3A^*, D^+A^-, and D^-A^+, are depicted in Figure 2. We use the Mulliken DA (donor–acceptor) terminology and arbitrarily denote the radical as D and the alkene as A. Thus, D^+A^- and D^-A^+ represent the charge-transfer configurations of the system, while D^3A^* signifies excitation of the alkene to its π triplet state.

A configuration-mixing diagram which demonstrates the way these configurations mix to generate a ground-state profile is shown schematically in Figure 3. For simplicity, it is assumed that just one of the charge-transfer configurations is involved (D^+A^- is arbitrarily chosen). According to the model, an approximate description of the transition state (TS) may be formally represented by the wave function depicted in eq 5.[20]

$$\psi_{TS} \approx (1 + \lambda^2)^{-1/2}\{2^{-1/2}[DA + D^3A^*] + \lambda\Phi_{CT}\} \quad (5)$$

Such a description assumes that the transition state lies in the immediate vicinity of the crossing point of reactant and product configurations and that just one charge-transfer configuration (labeled Φ_{CT}) mixes into the bonding combination of DA and D^3A^* with a mixing parameter, λ. This approach for describing

(19) For previous applications of the curve-crossing model to radical reactions, see: (a) Shaik, S. S.; Bar, R. *Nouv. J. Chim.* **1984**, *8*, 11. (b) Shaik, S. S.; Hiberty, P. C. *J. Am. Chem. Soc.* **1985**, *107*, 3089. (c) Pross, A. *Isr. J. Chem.* **1985**, *26*, 390. (d) Shaik, S. S.; Hiberty P. C.; Lefour, J. M.; Ohanessian, G. *J. Am. Chem. Soc.* **1987**, *109*, 363. (e) Shaik, S. S.; Canadell, E. *J. Am. Chem. Soc.* **1990**, *112*, 1446.

(20) Shaik, S.; Ioffe, A.; Reddy, A. C.; Pross, A. *J. Am. Chem. Soc.* **1994**, *116*, 262.

Table 2. Calculated Structural Parameters[a] Related to $CH_3^•$, $CH_2OH^•$, and $CH_2CN^•$ Addition Reactions to CH_2=CHX

	r(C–C)[b]			ϕ_{attack}[c]			ϕ_{pyr}[d]		
X	$CH_3^•$	$CH_2OH^•$	$CH_2CN^•$	$CH_3^•$	$CH_2OH^•$	$CH_2CN^•$	$CH_3^•$	$CH_2OH^•$	$CH_2CN^•$
F	2.246	2.226	2.173	109.9	108.2	109.3	25.0	25.9	28.0
H	2.246	2.222	2.177	109.1	108.7	107.4	21.8	22.3	24.5
NH_2	2.240	2.220	2.178	111.0	109.8	109.5	25.8	26.5	27.9
Cl	2.264	2.245	2.181	108.9	107.8	107.4	22.4	23.3	26.0
CHO	2.312	2.291	2.230	107.6	107.4	106.6	18.6	19.0	22.1
CN	2.313	2.287	2.219	107.5	107.2	106.4	19.0	19.4	23.7

[a] UHF/6-31G* values. [b] Length (Å) of the forming bond between the radical and the alkene in the transition structure (see Figure 1). [c] Angle of attack (deg) of the radical in the transition structure (see Figure 1). [d] Extent of pyramidalization (deg) at the proximal alkene carbon in the transition structure (see Figure 1).

Table 3. Calculated Barriers and Enthalpies Related to $CH_3^•$, $CH_2OH^•$, and $CH_2CN^•$ Addition Reactions to CH_2=CHX[a]

	barrier			enthalpy		
X	$CH_3^•$	$CH_2OH^•$	$CH_2CN^•$	$CH_3^•$	$CH_2OH^•$	$CH_2CN^•$
F	39.8	35.0	42.3	–94.2	–87.5	–63.2
H	38.9[b]	32.7	42.5	–93.5[c]	–87.1	–63.3
NH_2	36.3	32.5	30.7	–100.2	–91.4	–72.1
Cl	32.5	24.6	35.9	–105.9	–97.8	–74.5
CHO	28.7	18.3	33.9	–120.7	–118.6	–92.9
CN	24.3	11.7	32.6	–129.3	–123.7	–93.4

[a] QCISD/6-311G** + ZPE values, in kJ mol^{-1} (see text). [b] Experimental value, corrected to 0 K, is 38.2 kJ mol^{-1}, from ref 16. [c] Experimental value is 94.7 kJ mol^{-1}, from ref 17.

Table 4. Calculated Ionization Energies (I),[a] Electron Affinities (A),[a] and Energies (eV) of Charge-Transfer States (D^+A^- and D^-A^+)[b] Related to $CH_3^•$, $CH_2OH^•$, and $CH_2CN^•$ Addition Reactions to CH_2=CHX

			$CH_3^•$		$CH_2OH^•$		$CH_2CN^•$	
X	I[c]	A[d]	D^+A^-	D^-A^+	D^+A^-	D^-A^+	D^+A^-	D^-A^+
F	10.37	–1.62	11.39	10.33	9.05	10.51	11.78	8.78
H	10.58	–1.86	11.63	10.54	9.30	10.72	12.03	8.99
NH_2	8.18	–1.92	11.69	8.14	9.35	8.32	12.08	6.59
Cl	9.98		11.05[e]	9.94	8.71[e]	10.12	11.44[e]	8.39
CHO	10.21	0.03	9.74	10.17	7.46	10.35	10.13	8.62
CN	10.98	–0.23	10.00	10.94	7.66	11.12	10.39	9.39

[a] G2(MP2) adiabatic ionization energies (I) and electron affinities (A) of alkenes, in eV. [b] Charge-transfer energies of separated reactants, calculated from theoretical I and A values for $CH_3^•$, $CH_2OH^•$, $CH_2CN^•$, and CH_2=CHX. [c] G2(MP2) I values for $CH_3^•$, $CH_2OH^•$, and $CH_2CN^•$ are 9.77, 7.43, and 10.16 eV, respectively. Corresponding experimental values are 9.84, 7.56, and 10.0 eV, respectively, from ref 17. [d] G2(MP2) A values for $CH_3^•$, $CH_2OH^•$, and $CH_2CN^•$ are 0.04, –0.14, and 1.59 eV, respectively. Corresponding experimental values are 0.08 ($CH_3^•$) and 1.543–1.560 ($CH_2CN^•$) eV, from ref 17. [e] Calculated using experimental electron affinity for chloroethylene (–1.28 eV), from ref 18.

Table 5. Calculated Charge-Transfer[a] Data Related to $CH_3^•$, $CH_2OH^•$, and $CH_2CN^•$ Addition Reactions to CH_2=CHX

	Bader			Mulliken		
X	$CH_3^•$	$CH_2OH^•$	$CH_2CN^•$	$CH_3^•$	$CH_2OH^•$	$CH_2CN^•$
F	–0.012	0.014	–0.070	–0.004	0.035	–0.062
H	–0.017	0.005	–0.076	–0.011	0.023	–0.072
NH_2	–0.039	–0.019	–0.110	–0.033	0.003	–0.105
Cl	0.000	0.025	–0.055	0.007	0.045	–0.048
CHO	0.006	0.030	–0.050	0.013	0.048	–0.042
CN	0.012	0.039	–0.036	0.020	0.055	–0.029

[a] Amount of charge transfer (CT) from the radical to the alkene in the transition structure (UHF/6-31G*). A positive value indicates electron transfer from the radical to the alkene.

the transition state of an organic reaction has been shown to be useful for S_N2 ionic and Menschutkin reactions.[20] A more qualitative representation of eq 5 would be the resonance representation shown in eq 6, where Φ_{CT} is assumed to be D^+A^-:

$$TS = DA \leftrightarrow D^3A^* \leftrightarrow D^+A^- \quad (6)$$

A configuration-mixing description of the transition state allows us to assess the effect of perturbations (substituent or solvent) on the energy of the transition state. Specifically, the curve-crossing analysis suggests that if the charge-transfer configurations are high in energy so that the extent of mixing is small (i.e., small λ), then the height of the energy barrier will be primarily governed by the avoided crossing of reactant and product configurations. However, more generally, where a charge-transfer configuration is sufficiently low in energy that it contributes significantly to a description of the ground-state wave function (and hence the transition state), then this will manifest itself in two ways: (a) there will be a reduction in the energy barrier, and (b) the transition

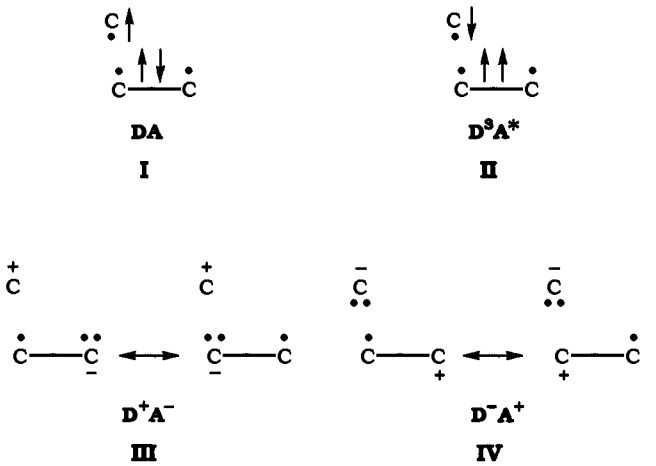

Figure 2. Principal configurations involved in the addition of substituted methyl radicals to alkenes.

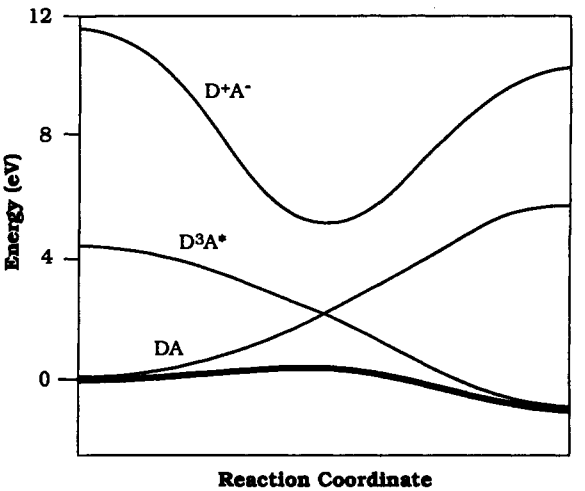

Figure 3. Curve-crossing diagram showing the mixing of DA, D^3A^*, and D^+A^- configurations in the schematic generation of the ground-state reaction surface (bold line) for the addition of methyl radical to monosubstituted ethylenes. The curves are drawn to correspond approximately to the energies (where available) for the system of methyl radical plus ethylene.

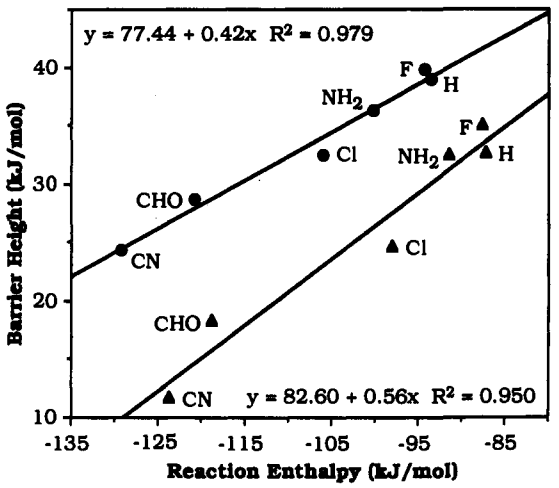

Figure 4. Plot of barrier height against reaction enthalpy (QCISD/6-311G** + ZPE, kJ mol^{-1}) for the addition of $CH_3^\bullet$ (●) and $CH_2OH^\bullet$ (▲) radicals to alkenes CH_2=CHX (X = H, NH_2, F, Cl, CHO, and CN).

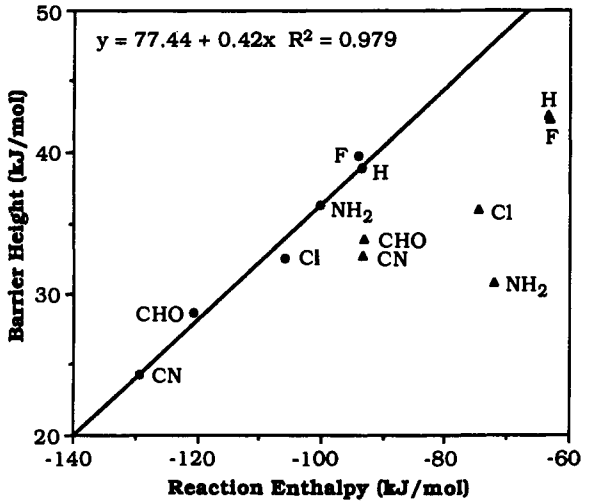

Figure 5. Plot of barrier height against reaction enthalpy (QCISD/6-311G** + ZPE, kJ mol^{-1}) for the addition of $CH_3^\bullet$ (●) and $CH_2CN^\bullet$ (▲) radicals to alkenes CH_2=CHX (X = H, NH_2, F, Cl, CHO, and CN).

state will take on the polar character associated with the particular charge-transfer configuration that has mixed in.

Effect of Reaction Enthalpy on Reactivity. A first step in assessing the importance of enthalpy on radical reactivity is to plot the dependence of barrier height on the enthalpy of reaction for a set of alkenes, using the results summarized in Table 3. This was carried out for each of the radicals, $CH_3^\bullet$, $CH_2OH^\bullet$, and $CH_2CN^\bullet$, in their reactions with CH_2=CHX (X = H, F, NH_2, Cl, CHO, and CN). The plots for $CH_2OH^\bullet$ and $CH_3^\bullet$ are compared in Figure 4, and the plots for $CH_2CN^\bullet$ and $CH_3^\bullet$ are compared in Figure 5. We note that the $CH_3^\bullet$ plots obtained in the present study at the QCISD/6-311G** + ZPVE level are very similar to those obtained in our previous study[5] at the QCISD(T)/6-311G** + ZPVE level.

The plot of barrier height versus enthalpy for $CH_2OH^\bullet$ gives a very good correlation (R^2 = 0.950), as also observed both here and previously[5] for $CH_3^\bullet$ (R^2 = 0.979). This might suggest that enthalpy is a key factor, possibly the dominant factor, in governing reactivity in the addition of $CH_2OH^\bullet$ radical to alkenes. However, as we will subsequently see, the true picture is more complex.

A second observation is that all the points for the $CH_2OH^\bullet$ correlation line lie *below* the $CH_3^\bullet$ correlation line. In other words, for a given reaction enthalpy the barrier for $CH_2OH^\bullet$ addition *is less than* that for $CH_3^\bullet$ addition. This observation by itself suggests some stabilizing factor in the $CH_2OH^\bullet$ addition mechanism (compared with $CH_3^\bullet$) and is confirmed by the subsequent analysis.

A third observation is the fact that the slope of the barrier–enthalpy correlation for $CH_2OH^\bullet$ (0.56) is significantly greater than that for $CH_3^\bullet$ (0.42). The traditional interpretation of barrier–enthalpy (or rate–equilibrium) slopes (normally represented by the Greek letter α) is that they provide information regarding the position of the transition state along the reaction coordinate.[21,22] Thus, the correlation slopes would suggest that the transition state for $CH_2OH^\bullet$ addition is relatively "late" along the reaction coordinate (large α) compared with that for $CH_3^\bullet$ addition (small α). We will subsequently see that this interpretation of the barrier–enthalpy slopes is invalid, and the difference in slopes has a different cause.

In contrast to the excellent barrier–enthalpy correlation exhibited by $CH_3^\bullet$ and $CH_2OH^\bullet$, a plot of barrier height versus enthalpy for the addition reactions of $CH_2CN^\bullet$ (Figure 5) shows total scatter. Clearly, in the case of $CH_2CN^\bullet$, enthalpy is *not* the dominant factor governing the barrier height. However, just as for $CH_2OH^\bullet$, all the points for the $CH_2CN^\bullet$ plot fall *below* the $CH_3^\bullet$ line, again suggesting some stabilizing factor that operates for $CH_2CN^\bullet$ addition compared with $CH_3^\bullet$ addition.

Effect of Polar Character on Reactivity. The curve-crossing model provides a framework for understanding the way in which the charge-transfer configurations, D^+A^- and D^-A^+, mix into the transition-state wave function. As described by eq 5 (and qualitatively by eq 6), the effect of such mixing is to stabilize the transition state and impart it with polar character. Our previous analysis for the addition of $CH_3^\bullet$ radical to alkenes led to the surprising conclusion that polar contributions to the energy of the transition state were small and that the dominant effect governing barrier height in the addition of $CH_3^\bullet$ to alkenes was reaction enthalpy.[5] There was no evidence for the prevalent view that the methyl radical is generally nucleophilic in character. We now wish to apply this analysis to the addition reactions of the two substituted methyl radicals, $CH_2OH^\bullet$ and $CH_2CN^\bullet$, and to compare the results with those obtained for the reactions of $CH_3^\bullet$ radical so that a more complete picture of the polar factor for $YCH_2^\bullet$ radical addition to alkenes can be generated.

The relative importance of possible charge-transfer contributions for a given system of a radical and an alkene may be assessed in two independent ways: (i) by estimating the energies of the D^+A^- and D^-A^+ configurations from the ionization energy (I) and electron affinity (A) values of the radical and alkene at infinite separation and (ii) from the computed charge distribution within the transition state for radical addition.

Our calculated ionization energies and electron affinities for the $YCH_2^\bullet$ radicals and CH_2=CHX alkenes, as well as the energies of the D^+A^- and D^-A^+ configurations at infinite separation, are listed in Table 4. Inspection of these data reveals that for most $CH_2OH^\bullet/CH_2$=CHX reactant pairs (i.e. for X = F, H, Cl, CHO, and CN), the energy of D^+A^- is lower than that of D^-A^+. In other words, $CH_2OH^\bullet$ is likely to exhibit *nucleophilic* character toward five of the six alkenes studied. It is only with the strong electron-donating substituent, X = NH_2, that D^-A^+ lies lower in energy than D^+A^-, so on this basis it is only toward CH_2=$CHNH_2$ that $CH_2OH^\bullet$ would be expected to exhibit *electrophilic* character.[23]

The second approach for assessing polar character in the radical addition reactions is to analyze charges in the transition states. We do this using both Bader[12] and Mulliken methods, and the relevant data are shown in Table 5. For the same five substituted ethylenes (X = F, H, Cl, CHO, and CN), the Bader charges

(21) (a) Leffler, J. E.; Grunwald, E. *Rates and Equilibria of Organic Reactions*; Wiley: New York, 1963. (b) Leffler, J. E. *Science* **1953**, *117*, 340. (c) Jencks, W. P. *Chem. Rev.* **1985**, *85*, 511, and references therein.

(22) For a questioning of the validity of the Leffler principle, see: Pross, A.; Shaik, S. S. *New J. Chem.* **1989**, *13*, 427, and references therein.

indicate that the transfer of charge in the transition states takes place *from* the $CH_2OH^•$ radical *to* the alkene, while for X = NH_2 the direction of charge-transfer is reversed. The picture from the Mulliken charges is essentially the same except that for X = NH_2 the charge transfer is effectively zero. So both procedures lend support to the conclusion that $CH_2OH^•$ is generally a nucleophilic radical.

Let us now consider the polar character in the addition reactions of $CH_2CN^•$. We see from Table 4 that for all six alkenes in the study D^-A^+ lies lower in energy than D^+A^-; that is, $CH_2CN^•$ is likely to exhibit *electrophilic* properties toward the entire set of alkenes. This conclusion is reinforced by examination of the transition-state charges (Table 5) with both Bader and Mulliken procedures; for all six alkenes there is a transfer of charge from the alkene to the radical.

The above analysis indicates the direction and extent of charge transfer, but does not reveal the energetic consequences. To what extent does mixing of D^+A^- or D^-A^+ into the wave function stabilize the transition state for $CH_2OH^•$ and $CH_2CN^•$ addition to alkenes? Or put differently, how important are polar effects in governing reactivity for $CH_2OH^•$ and $CH_2CN^•$ addition?

Inspection of the data in Table 4 makes it apparent that in almost every case the lower energy charge-transfer configurations for $CH_2OH^•$ (normally D^+A^-) and $CH_2CN^•$ (normally D^-A^+) lie significantly lower, relative to the ground state, than the corresponding lower energy charge-transfer configurations for $CH_3^•$ (either D^+A^- or D^-A^+ depending on the substituent). This suggests that charge-transfer character will be more pronounced in reactions of both $CH_2OH^•$ and $CH_2CN^•$ than in those of $CH_3^•$. However, it still does not tell us whether there is significant polar stabilization of the transition state in the reactions of $CH_2OH^•$ and $CH_2CN^•$ with alkenes. Let us therefore explore this aspect now.

Polar Effects in $CH_2OH^•$ Addition. If polar effects are dominant in $CH_2OH^•$ and $CH_2CN^•$ addition, then this may become apparent from a correlation between barrier height and alkene electron affinity in the case of the nucleophilic radical, $CH_2OH^•$, and between barrier height and ionization energy for the electrophilic radical, $CH_2CN^•$.

A plot of barrier height versus alkene electron affinity for $CH_2OH^•$ addition to CH_2=CHX is shown in Figure 6. A reasonable correlation is observed (R^2 = 0.839). Thus, we find that for $CH_2OH^•$ the barrier height correlates with both reaction enthalpy (Figure 4) *and* with alkene electron affinity (Figure 6). This behavior has been previously noted for the 2-cyanopropyl radical[2d] and was also observed in our earlier study of the methyl radical.[5]

The fact that both parameters correlate with barrier height does not necessarily mean that both parameters affect reactivity; it merely tells us that the two parameters are not independent but correlate with one another. Consequently, we must find a way of separating these two factors so that we can discover whether it is one or both that is actually responsible for governing reactivity.

In the case of methyl radical addition it was concluded, based on a detailed charge analysis, that the primary correlation was between barrier height and enthalpy and that the correlation between barrier height and electron affinity was fortuitous and due to a correlation between enthalpy and electron affinity for the systems examined.[5] For the case of $CH_2OH^•$, a separation of polar and enthalpy effects in the way that was carried out for

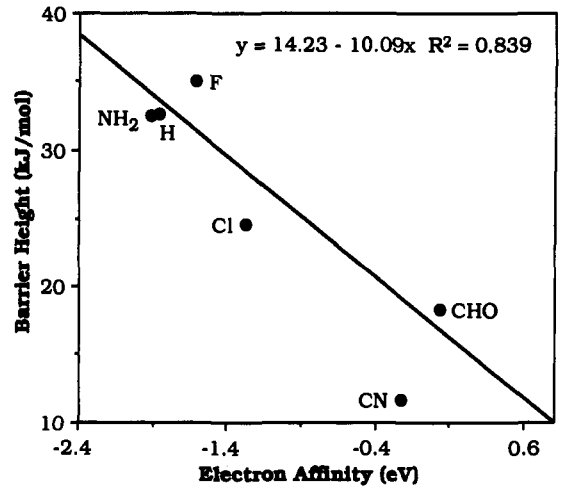

Figure 6. Plot of barrier height (QCISD/6-311G** + ZPE, kJ mol^{-1}) against alkene electron affinity (G2(MP2), eV) for the addition of $CH_2OH^•$ radical to alkenes CH_2=CHX (X = H, NH_2, F, Cl, CHO, and CN).

$CH_3^•$ is not possible; the charge analysis demonstrates that $CH_2OH^•$ is generally nucleophilic toward alkenes, so that it is not immediately obvious whether the barrier height correlation stems from a charge-transfer stabilization of the transition state or from an enthalpy-derived stabilization.

A way to resolve this dilemma is to compare the $CH_2OH^•$ barrier–enthalpy plot with the corresponding plot for $CH_3^•$ (Figure 4). Since we concluded that for $CH_3^•$ addition polar effects on the barrier height were small, *we can use the methyl plot as a reference, representing radical addition reactions that are enthalpy dominated.* In this light, the barrier height–enthalpy correlation for $CH_2OH^•$ in Figure 4 takes on new significance.

We have already noted that the correlation line for $CH_2OH^•$ is lower than the one for $CH_3^•$. In other words, for any given reaction enthalpy, the barrier for $CH_2OH^•$ addition is *smaller* than that for $CH_3^•$ addition. The energy difference ranges from about 5 kJ mol^{-1} to about 15 kJ mol^{-1}. *We propose that this energy gap between the two lines is largely due to polar stabilization of the transition state.* Consistent with this interpretation, the gap is larger in the region of strong electron-withdrawing substituents on the alkene (CHO and CN) where D^+A^- is strongly stabilized, and the polar character would be large, but the energy gap is smaller in the region of other substituents for which the energy of D^+A^- is higher.

A curve-crossing analysis of the addition reactions of $CH_2OH^•$ supports the above conclusions. In our recent study of $CH_3^•$ addition, it was pointed out that for the $CH_3^•$ addition reaction to ethylene the low-energy charge-transfer configuration, D^-A^+, was at least 4.4 eV above the reactants and probably 2–3 eV above the crossing point of DA and D^3A^* (see Figure 2).[5] This relatively large energy gap precluded significant mixing of D^-A^+ into the transition-state wave function in this particular case.

If we now examine the energies of the charge-transfer configurations for the $CH_2OH^•/CH_2$=CHX pairs (Table 4), we find that, with the exception of X = NH_2, the energies of the lower lying configuration are significantly less than the corresponding values for $CH_3^•$ (by 1.2–2.3 eV). This brings the charge-transfer configurations substantially closer in energy to the crossing point and allows them to mix into the transition-state wave function to a greater extent.[23]

We conclude that *the barrier to $CH_2OH^•$ addition is generally influenced by both polar and enthalpy factors and that the importance of the polar factors increases as the acceptor ability of the alkene increases.* The magnitude of the polar stabilization (ca. 5–15 kJ mol^{-1}) means that polar stabilization in this system can lead to rate enhancements of close to 3 orders of magnitude.

(23) The fact that the energy of D^-A^+ for the $CH_3^•CH_2$=$CHNH_2$ pair is low (8.14 eV) and slightly lower than for the $CH_2OH^•/CH_2$=$CHNH_2$ pair (8.32 eV) is interesting. It suggests that there may be slight polar stabilization for $CH_3^•$ addition to CH_2=$CHNH_2$. However, the situation for CH_2=$CHNH_2$ is complicated by the fact that ionization removes an electron from an orbital associated to a significant extent with the nitrogen lone pair (rather than just the ethylenic double bond), and so the appropriateness of the calculated ionization energy in the evaluation of the D^-A^+ energy is not entirely clear. As can be seen from Table 4, the energies of the D^+A^- and D^-A^+ configurations for the $CH_3^•$ radical addition reactions with other alkenes are all relatively high, so that polar contributions in $CH_3^•$ addition to alkenes appear in general to be small and energetically not significant.

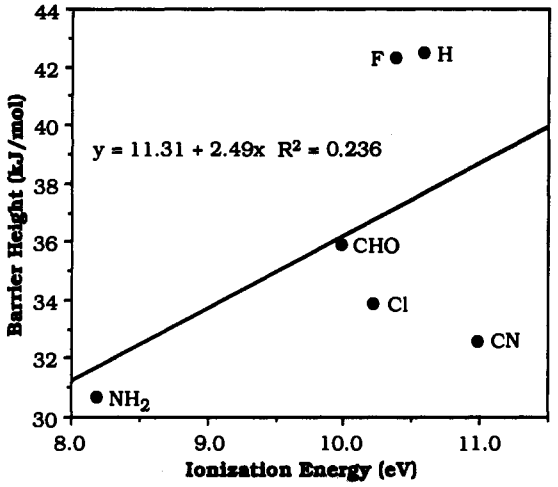

Figure 7. Plot of barrier height (QCISD/6-311G** + ZPE, kJ mol^{-1}) against alkene ionization energy (G2(MP2), eV) for the addition of $CH_2CN^•$ radical to alkenes CH_2=CHX (X = H, NH_2, F, Cl, CHO, and CN).

Furthermore, the larger slope of the $CH_2OH^•$ barrier–enthalpy plot compared with the $CH_3^•$ barrier–enthalpy plot is *not* indicative of a "later" transition state for $CH_2OH^•$, but arises from the growing contribution of transition-state stabilization from polar mixing (from D^+A^-) for alkenes with the more electron-withdrawing substituents (CHO and CN). *This growing polar contribution with increasing alkene electron affinity fortuitously preserves the linearity of the barrier height–enthalpy plot.*

Polar Effects in $CH_2CN^•$ Addition. A plot of barrier height for $CH_2CN^•$ addition versus alkene ionization energy is shown in Figure 7. It is apparent that there is no correlation between these two parameters. We must conclude, therefore, that polar contributions to $CH_2CN^•$ addition are not the *dominant* factor in governing reactivity in this reaction. We have already seen a lack of correlation in the barrier height–enthalpy plot (Figure 5), indicating that enthalpy is also not the dominant factor. Thus, neither enthalpy nor polar factors *on their own* dominate the reactivity of the $CH_2CN^•$ radical toward alkenes. In order to assess whether the reactivity is influenced by a *combination* of enthalpy and polar factors, we need to analyze the barrier height–enthalpy and barrier height–ionization energy plots in more detail.

In the barrier height–enthalpy plot for $CH_2CN^•$ (Figure 5), it is the point for X = NH_2 that primarily upsets the linear correlation: the barrier for addition to CH_2=$CHNH_2$ is substantially lower (by approximately 10 kJ mol^{-1}) than that for addition to ethylene or CH_2=CHF, despite the fact that the enthalpies of reaction are similar. Inspection of the charge-transfer energies (Table 4) makes the reason for this failure clear. The energy of D^-A^+ for $CH_2CN^•$ addition to CH_2=$CHNH_2$ is especially low (6.59 eV), so that there is substantial mixing of this configuration into the TS wave function with consequent TS stabilization. So despite the relatively low exothermicity of this reaction, the barrier to addition is also relatively low.

Turning to the ionization energy plot (Figure 7), we see that it is now the point for X = CN that shows the greatest deviation from a barrier–ionization energy correlation. The barrier for addition to CH_2=CHCN is significantly lower than what would be expected based on a barrier–ionization energy correlation alone. Thus, despite CH_2=CHCN having an ionization energy similar to ethylene and CH_2=CHF, the barrier for $CH_2CN^•$ addition to CH_2=CHCN is substantially lower (by ca. 10 kJ mol^{-1}). The reason for the low barrier is that the exothermicity of $CH_2CN^•$ addition to CH_2=CHCN is much greater than that for addition to ethylene or CH_2=CHF, and this results in a lower barrier than would be expected from ionization energy considerations alone.

We conclude that, *in the addition of CH_2CN to alkenes, both enthalpy and polar effects are important, so that a good correlation with either parameter alone is not found.*

If, once again, we treat the addition of $CH_3^•$ as a reference reaction for an enthalpy-governed process with little polar character, we observe that all the points for the $CH_2CN^•$ addition lie *below* the $CH_3^•$ barrier height–enthalpy plot (Figure 5). This observation reinforces our view that for $CH_2CN^•$ addition there are significant polar contributions that lower the energy barrier compared with those that would be expected based on enthalpy considerations alone. Again we might consider the vertical deviation from this line as an approximate measure of the degree of polar stabilization in the transition state. Consistent with this, the point for CH_2=$CHNH_2$, with a particularly low-energy D^-A^+ configuration (6.59 eV), deviates much more than the other points from the $CH_3^•$ correlation line. Thus, from Figure 5, it appears that polar stabilization energies for $CH_2CN^•$ range up to ca. 15 kJ mol^{-1}.

The curve-crossing analysis supports this conclusion. The energies of the preferred charge-transfer configuration for $CH_2CN^•$ addition, D^-A^+, are substantially lower than the corresponding energies for $CH_3^•$ addition (Table 4), in each case by ca. 1.5 eV. This lowering of the D^-A^+ energy so that it is closer to the crossing-point energy facilitates its mixing into the transition-state wave function, thereby stabilizing the transition state and imparting it with charge-transfer character.

The above analysis enables us to estimate roughly at what energy a charge-transfer configuration is likely to lead to transition-state stabilization. From Table 4 and the energy plots of Figures 4 and 5, we conclude that energetically significant polar contributions to the transition state of $YCH_2^•$ addition to alkenes begin to appear *when the energy relative to reactants of one of the charge-transfer configurations drops below ca. 9–9.5 eV.*

Characterization of the Transition State. The existence of a correlation between rates and equilibria (or between barrier height and reaction enthalpy) for many chemical reactions is quite general, though by no means universal.[21] When such a correlation does exist, the slope of the correlation line, labeled α, is often found to lie in the range 0–1 and is commonly considered to measure the position of the transition state along the reaction coordinate. The existence of such correlations forms the basis of the Leffler principle, which considers the transition state to be intermediate in character between reactants and products.[21,22]

Whereas two of the radicals ($CH_2OH^•$ and $CH_3^•$) generate individual barrier height–enthalpy correlations, we have seen that $CH_2CN^•$ fails to do so. Not surprisingly, if one combines the results for all three sets of radical addition reactions into a single barrier height–enthalpy plot, no overall correlation is found; the plot that is observed is one of total scatter.

Interestingly, when one plots the incipient C–C bond length in the transition state (listed in Table 2) against reaction enthalpy for the three sets of reactions, a remarkably good correlation, illustrated in Figure 8, is observed (R^2 = 0.953). What is the significance of a correlation of bond length against reaction enthalpy that covers the reactions of *all three radicals*, whose mechanistic character we have seen to be distinctly different? And why is there no corresponding correlation between barrier height and reaction enthalpy for the set of three radicals? A description of the transition state in terms of the curve-crossing model provides a simple explanation both for the bond length–enthalpy correlation and for the absence of a barrier height–enthalpy correlation and provides some general insights into those parameters that are more likely to correlate with one another.

The curve-crossing model suggests that the position of the transition state is likely to be located close to the crossing point of the reactant and product configurations (in this case DA and D^3A^*). Indeed, this hypothesis has been shown to hold for ionic

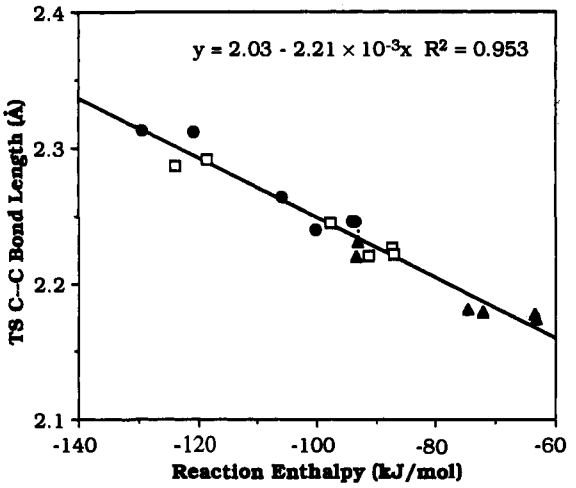

Figure 8. Plot of C–C bond length in the transition state (UHF/6-31G*, Å) against reaction enthalpy (QCISD/6-311G* + ZPE, kJ mol^{-1}) for the addition of $CH_3^•$ (●), $CH_2OH^•$ (□), and $CH_2CN^•$ (▲) radicals to alkenes CH_2=CHX (X = H, NH_2, F, Cl, CHO, and CN).

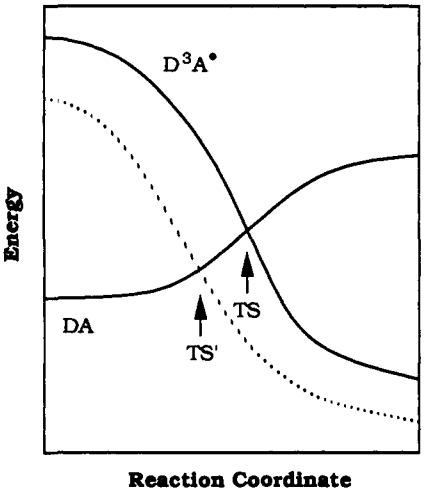

Figure 9. Schematic diagram showing the effect of a substituent that lowers the energy of the product configuration D^3A^* (unbroken line without the substituent, broken line with the substituent) in the addition reaction of substituted methyl radicals to alkenes.

and Menschutkin S_N2 reactions.[20] Interestingly, the geometry of the crossing point and that of the transition state were found to be close even when a third configuration, the so-called intermediate configuration, mixes into the transition-state wave function. So it appears that mixing in of a third configuration can have a significant effect on the transition-state *energy* and *charge distribution* without significantly shifting the *position* of the transition state.

The observed correlation between TS bond length and reaction enthalpy and the lack of correlation between barrier height and enthalpy for $YCH_2^•$ addition can now be understood in these terms. In our earlier work on methyl radical addition reactions,[5] we pointed out that the reaction enthalpy is governed by the energy of the D^3A^* configuration. Thus, lowering the energy of the entire D^3A^* curve increases the reaction exothermicity and leads to an earlier crossing point (in structural terms) and hence an earlier transition state (from TS to TS'), i.e, a longer C(radical)–C(alkene) bond in the transition state (Figure 9). The reason for the transition-state structure–reaction enthalpy correlation in radical addition reactions then becomes clear: the position of the transition state along the reaction coordinate (governed by the DA–D^3A^* crossing point) and the energy of the products (governed by the D^3A^* curve in the product geometry) are directly linked.[24]

The *absence* of a barrier height–enthalpy correlation that extends over all three radicals may be attributed to the great variation in the extent of charge-transfer contributions to the transition state in these radical addition reactions: it is largely absent for $CH_3^•$, while present to varying extents for $CH_2OH^•$ and $CH_2CN^•$. Since in many cases these polar contributions affect the energy of the transition state without affecting the energy of the radical product, the linkage between barrier height and reaction enthalpy is effectively broken. For this reason, no overall barrier height–enthalpy correlation is observed for the set of three radicals.

Of course one might anticipate that, in cases where the energy of the charge-transfer configuration is stabilized even more strongly (with radical–alkene systems that constitute even better DA pairs), the observed correlation between transition-state structure and reaction enthalpy will eventually break down. Clearly a point must be reached where very extensive mixing of the charge-transfer configuration into the ground-state wave function will affect not only the transition-state energy but its structure as well. When this point is reached, the location of the transition state and the crossing point of DA and D^3A^* will no longer coincide and the observed correlation between transition-state structure and reaction enthalpy will break down. This situation is currently being explored.

Finally, since this study and others demonstrate that radical addition transition states often possess charge-transfer character, we must conclude that the Leffler postulate,[21] which assumes the transition state to be intermediate in character between reactants and products, is not applicable to radical addition reactions. As a corollary, the slope of barrier height–enthalpy (or rate–equilibrium) correlations in radical addition reactions *cannot* be taken as a measure of transition-state structure.[22] This conclusion necessarily raises further doubt as to the validity of the Leffler postulate for other reactions.

Conclusions

This theoretical study of the addition reaction of $CH_3^•$, $CH_2OH^•$, and $CH_2CN^•$ radicals to alkenes in the gas phase leads to the following conclusions.

(1) The reactivity of the $CH_3^•$ radical is primarily governed by enthalpy effects. Given that the $CH_3^•$ radical is both a weak electron donor and a weak electron acceptor, the charge-transfer configurations (D^+A^- and D^-A^+) associated with $CH_3^•$ addition tend to be relatively high in energy and normally do not mix significantly into the transition-state wave function.

(2) In contrast to the $CH_3^•$ radical, the reactivities of the $CH_2OH^•$ and $CH_2CN^•$ radicals are strongly influenced by polar effects and not just by enthalpy effects. $CH_2OH^•$ generally exhibits nucleophilic behavior, while $CH_2CN^•$ generally exhibits electrophilic behavior. For a given reaction enthalpy, the polar character of the transition states for $CH_2OH^•$ and $CH_2CN^•$ addition lowers the barrier heights for these two radicals compared with $CH_3^•$. This polar stabilization is particularly pronounced for the $CH_2OH^•/CH_2$=CHCN pair and for the $CH_2CN^•/CH_2$=$CHNH_2$ pair (each ca. 15 kJ mol^{-1}).

(3) The absence of a general barrier height–enthalpy correlation (equivalent to a rate–equilibrium correlation) for the three radicals, $CH_3^•$, $CH_2OH^•$, and $CH_2CN^•$, is due to the mixing into the transition state of charge-transfer character for $CH_2OH^•$ and $CH_2CN^•$, which stabilizes the transition state without correspondingly affecting the reaction enthalpy. It would appear

(24) We note, as an aside, that the angular structural parameters in the transition state, ϕ_{attack} and ϕ_{pyr}, correlate reasonably well with r(C–C) (Table 2) and also reflect the early/late character. Thus, the angle of attack (ϕ_{attack}) of the radical varies from slightly less than the tetrahedral value for earlier transition states to slightly greater than the tetrahedral value for later transition states. Likewise, the degree of pyramidality (ϕ_{pyr}) at the proximate alkene carbon increases with increasing lateness of the transition state.

therefore that rate–equilibrium relationships may not be observed where an intermediate configuration contributes significantly to the description of the transition state.

(4) For the two cases where barrier height–enthalpy correlations are observed ($CH_3^•$ and $CH_2OH^•$), the slope of the correlation line is not a measure of the position of the transition state along the reaction coordinate, raising further doubts regarding the validity of this widely accepted idea.

(5) The observation of a general transition-state structure–enthalpy correlation (Figure 8) suggests that, in structural terms, the transition state for these radical addition reactions is located close to the intersection point of reactant and product configurations. A transition-state description that derives from the curve-crossing model provides a simple explanation for this correlation and predicts the circumstances under which it may break down.

Acknowledgment. Useful discussions with Professor Hanns Fischer, a generous allocation of time on the Fujitsu VP-2200 of the Australian National University Supercomputer Facility, and the awards of an ARC Senior Research Fellowship to A.P., and an Australian Research Fellowship to M.W.W. are gratefully acknowledged.

Supplementary Material Available: Geometries optimized at the UHF/6-31G* level for the species involved in the addition of $CH_2OH^•$ and $CH_2CN^•$ radicals to the $CH_2{=}CHX$ alkenes (X = H, NH_2, F, Cl, CHO, and CN) (8 pages). This material is contained in many libraries on microfiche, immediately follows this article in the microfilm version of the journal, and can be ordered from the ACS; see any current masthead page for ordering information.